Scientific Research Publishing

World Journal of Engineering and Technology, 2025, 13(3), 622-643
https://www.scirp.org/journal/wjet
ISSN Online: 2331-4249
ISSN Print: 2331-4222

MCNP Simulation of Multi-Capsule Irradiation Protocol for a K0-Based INAA Using the GHARR-1 MNSR

George Adu-Okyere[1], Vincent Yao Agbodemegbe[1], Isaac Kwasi Baidoo[1,2], Henry Cecil Odoi[1,2], Edward Shitsi[1,2,3*]

[1]Department of Nuclear Engineering, School of Nuclear and Allied Sciences, College of Basic and Applied Sciences, University of Ghana, Accra, Ghana
[2]National Nuclear Research Institute, Ghana Atomic Energy Commission, Accra, Ghana
[3]Nuclear Power Institute, Ghana Atomic Energy Commission, Accra, Ghana
Email: dsirgeorge@gmail.com, vincevalt@googlemail.com, baidooisaac51@yahoo.co.uk, hencilod@gmail.com, *edwardshitsi@yahoo.com

How to cite this paper: Adu-Okyere, G., Agbodemegbe, V.Y., Baidoo, I.K., Odoi, H.C. and Shitsi, E. (2025) MCNP Simulation of Multi-Capsule Irradiation Protocol for a K0-Based INAA Using the GHARR-1 MNSR. *World Journal of Engineering and Technology*, **13**, 622-643.
https://doi.org/10.4236/wjet.2025.133040

Received: July 15, 2025
Accepted: August 19, 2025
Published: August 22, 2025

Abstract

The GHARR-1 MCNP5 input deck was successfully modified to simulate the multi capsule irradiation protocol adopted in the present work to experimentally characterise the neutron flux in the inner irradiation channel of the GHARR-1 LEU core. The inner irradiation site was modified by discretising its 17cm active length into spatial demarcations to enable Bottom, Middle and Top irradiation other than the single capsule irradiation which is the normal protocol in the conduct of neutron activation analysis at the GHARR-1. Flux characterization and analytical measurement of sample were carried out in the three (3) irradiation capsules introduced into the inner irradiation channels at the bottom (normal), middle and top positions using the scheme developed in the experimental work for validation of the MCNP simulations. Flux monitors were used for irradiation and k0-method was adopted for the experimental flux characterization analysis. Neutron spectrum parameters such as Cadmium ratios, a measure of the deviation of epithermal neutrons from the ideal 1/E distribution (α) and thermal-epithermal flux ratio (f) were determined for the three capsules as well as the thermal, epithermal and fast neutron fluxes, and the MCNP simulation results were compared with these experimental results. Results obtained from the MCNP simulations agree fairly with experimental results. However, relatively high thermal, epithermal and fast neutron fluxes were obtained from the MNCP simulations than what was determined experimentally. This increase could be attributed to the treatment of the core as a fresh core for the MCNP simulation rather than a core that has been in

operation for five years with anticipated core depletion which may have impacted the experimental results. The present work could further be improved by incorporating results from burn up studies into the MCNP input deck so as to more appropriately capture and simulate the actual state of the GHARR-1 LEU core which has been in operation for almost 5 years.

Keywords

Neutron Spectrum Parameters, K0-Method, MCNP Simulation, Bottom, Middle and Top Irradiation Column, Flux Monitor

1. Introduction

MCNP Code and Modelling

Monte Carlo Neutron-Particle code (MCNP) is a class of computational algorithms that uses repeated random sampling to compute their results. For computations involving particle transport calculations such as neutrons, electrons and photons, the Monte Carlo computer code provides an extremely effective and flexible platform for parametric determination. The MCNP code is used for the computations of multiplication factors, reaction rates, saturated activities, neutron fluxes and spectra, power peaking factors, reaction rate distributions, shielding, among others. At almost all energies, MCNP can track 34 different particle types, including photons, light ions, 2000+ heavy ions, and nucleons. In cases when libraries are not accessible, it employs conventional or standard assessed data libraries combined with physics models [1] [2]. Different versions of the MCNP software exist which include MCNP5, MCNP6 and MCNPX developed at the Los Alamos Scientific Laboratory, USA. However, their functions are similar and work on the same principles. One can decide which one to use based on convenience. To be able to perform MCNP simulation, the user first creates an input file (deck) that is subsequently read by MCNP. This file contains information about the problem in areas such as the geometry specification, the description of materials and selection of cross-section evaluations, the location and characteristics of the neutron, photon, or electron source, the type of answers or tallies desired, and any variance reduction techniques used to improve efficiency.

The capability to handle complex geometry is a key benefit of using MCNP [2]. The MCNP employs these input cards: cell, surface and data cards format to define or modify the problem geometry (in this instance, a research reactor) and its material requirements. The surface cards are the fundamental building block of the problem geometry [1]-[4]. The different surfaces, including planes, cylinders, cones, spheres, among others, as well as their dimensions and orientation in the x, y, and z coordinate systems are all specified. A positive integer is used to identify each surface card (surface number). Cells are formed by combining operators using the intersection, union, and complement. These cells are described by the cell card, which

also determines the density, particle or photon importance, and material composition (via material number) of the cell (importance of 0 means, particle history is not followed in the cell while the importance of 1 means is the vice versa). To identify between the various material cards, a material number is used. In this work, while we used an existing MCNP model of the GHARR-1 Miniature Neutron Source Reactor (MNSR) core [3], we integrated into the model the cell cards for the irradiation capsules, tally cards, energy bins, etc., to replicate the experimental geometry.

Tallying in MCNP allows the user to define the output or information desired from the calculation and how this information is presented in the output file. MCNP offers seven common tally types (Briesmeister, 2005) [4]. Except for KCODE criticality situations, which are normalized to one fission neutron, all tallies are normalized to one "starting" particle and therefore one must employ the proper scaling factors to normalize the result by the thermal power of a system (reactor). The scaling factor can be applied at a later time during data processing or entered on the FM (tally multiplier) card. The cell flux tally (Fn), tally segment (FSn), tally multiplier (FMn) and tally energy (En) cards were employed as supplemental tally cards in this investigation. To be able to tell whether the output of a deck is usable depends on its output multiplication factor value (k-effective, k_{eff}). It is described as the proportion of a generation's neutron population to that of the generation before it. The kcode card in MCNP regulates criticality calculations. A generation is referred to as a k_{eff} cycle when used with the kcode card. Three input parameters are needed for the kcode card in MCNP: the total number of k_{eff} cycles, the starting k_{eff} guess, and the number of initial cycles to be skipped. Since the Monte Carlo spatial neutron distribution, which depends on the eigenvalue and geometry of the system of interest takes some time to converge, certain cycles must be skipped. The final estimate of the k_{eff} is presented as the average of all the simulated k_{eff} cycles at the end of an MCNP simulation. The final estimate of the k_{eff} has associated uncertainty, as with every Monte Carlo simulation. As the number of k_{eff} cycles increases, the uncertainty reduces. Therefore, it is crucial to simulate a significant number of k_{eff} cycles to obtain an accurate estimate of the final k_{eff} of a critical system [5]-[23].

MCNP simulation was employed in the present work and the results obtained from the MCNP simulation were compared with that of an experimental study on flux characterization in which a multi-capsule scheme realised through the introduction of three (3) irradiation capsules each of length 5 cm into the 23 cm long irradiation channel of the Ghana Research Reactor 1 (GHARR-1) facility was carried out. In addition to the experimental and MCNP characterization of the neutron parameters, the present study intended to highlight the differences in neutronics characteristics (*i.e.*, physics) of LEU and the HEU and also relate observations from the present study to that outlined by [23].

2. Ghana Research Reactor-1 (GHARR-1)

Ghana Research Reactor-1 (GHARR-1) with 34 kW reactor power and 13% enrichment is primarily utilized in the studies of reactor physics, nuclear engineer-

ing, nuclear reaction cross-section measurements and neutron activation analysis, among others. The current installed Low Enriched Uranium core (34 kW MNSR) is a converted Highly Enriched Uranium core (90.2%, 30 kW MNSR) [24]. It has been roughly six (6) years since the conversion was carried out and recent observations and measurements of neutron flux have revealed some distinctive variations in some of the neutron flux parameters as compared to the HEU core, particularly those reported in [23]. To provide experimenters with the most accurate spectral characteristics of experimental sites and to maintain a high degree of reliable information to carry out reactor experiments and most importantly neutron activation analysis, neutron spectrum characterization of GHARR-1 is the focus of this research work using MCNP simulation.

The GHARR-1 originally operated on a highly enriched uranium fuel core. However, as part of the US Department of Energy's project on Reduced Enrichment for Research and Test Reactors [25], it was transitioned from high-enriched uranium (HEU) to a low-enriched uranium (LEU) core. The GHARR-1 facility successfully undertook the core conversion in 2017. The reactor's maximum thermal neutron flux is 1.0×10^{12} ncm^{-2}·s^{-1}. The GHARR-1 facility is used basically for education and training and also for neutron activation analysis.

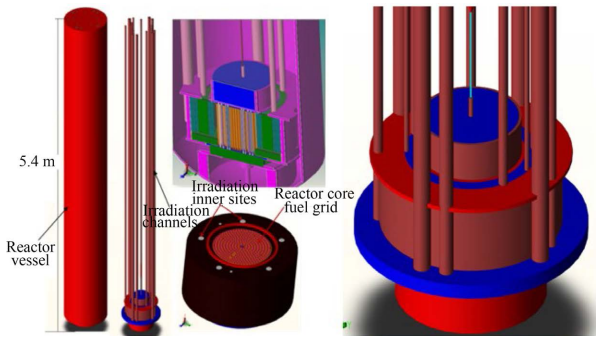

(A)

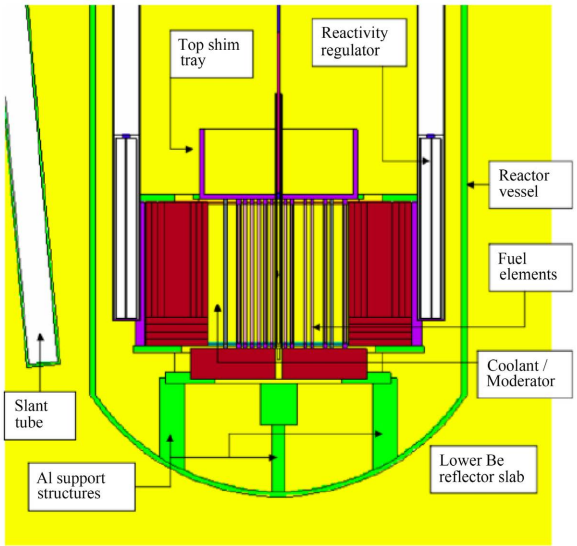

(B)

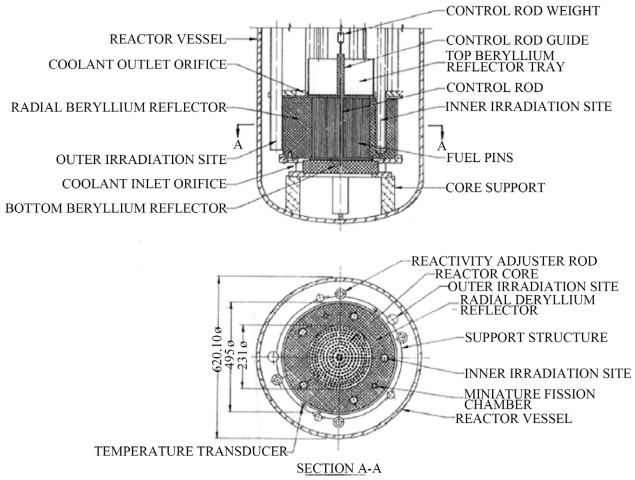

(C)

Figure 1. GHARR-1 LEU Core Reactor Components (A), MCNP5 plot of vertical cross section of the GHARR-1 model (B) and Cross-section through the GHARR-1 reactor (C).

The main components of the GHARR-1 reactor and the cross-section through the reactor used in the present study are as depicted in **Figures 1(A)-(C)** respectively. Comparison of key parameters for reference GHARR-1 HEU and LEU cores are shown in **Table 1**.

Table 1. Comparison of key parameters for reference GHARR-1 HEU and LEU cores [24].

Key Parameters	HEU	LEU
Reactor type	MNSR	MNSR
Fuel type	rod	rod
Power, kW	30	34
Fuel rod lattice	350	350
Number of Active Fuel rods	344	335
Number of Dummy rods	6	15
Core diameter (mm)	230	230
Core height (mm)	230	230
Fuel lattice pitch (mm)	10.95	10.95
Coolant inlet pressure (atm)	1	1
Coolant heat transfer mode	Natural convection	Natural Convection
Reflector	Beryllium	Beryllium
Control rod absorber	Cadmium	Cadmium
Control rod cladding	Stainless steel	Stainless steel
Number of control rods	1	1
Core shape	Cylindrical	Cylindrical
Coolant/moderator	Deionised water	Deionised water
Fuel Meat	U-Al_4	UO_2
U-235 Total Core Loading, g	~998.1	~1355.3
U-235 Enrichment, wt%	90.2	13.0
U-234 content, wt%	1.0	0.2

Continued

U-236 content, wt%	0.5	0.25
Density of Meat, g/cm^3	3.456	10.6
Meat Diameter, mm	4.3	4.3
Cladding Diameter, mm	5.5	5.5
Thickness of He Gap, mm	None	0.05
Cladding Material	Al-303-1	Zirc-4
Material for Grid Plates	LT-21	Zirc-4
Top Shim Tray	LT-21	LT-21
Material for Dummy Elements	Al-303-1	Zirc-4
Number of Tie Rods	4	4
Material for Tie Rods	Al-303-1	Zirc-4
Adjuster Guide Tubes	4	4
Effective Delayed Neutron Fraction	8.08×10^{-3}	8.57×10^{-3}
Prompt neutron lifetime (s)	8.12×10^{-5}	1.41×10^{-4}
Maximum thermal Neutron flux, n/cm^{2}s	1×10^{12}	1×10^{12}
Excess reactivity, mk	4.0	3.87
Control rod worth, mk	7.0	6.90
Shutdown margin, mk	3.0	3.03

3. Methodology

3.1. Experimental

3.1.1. Multi Capsule Irradiation Protocol for Flux Characterisation

Table 2 and Figure 2 show the experimental scheme adopted for flux characterization along the 15 cm length of the 17 cm active length of the inner irradiation channel in the GHARR-1 (The irradiation tube (or irradiation channel) covers the active length of 17 cm of the reactor. The length of the reactor core is 23 cm). Detailed theory and experimental procedure on Multi Capsule Irradiation Protocol for Flux Characterisation have been presented in the publication by Adu-Okyere *et al.* [26].

Table 2. Multi-capsule irradiation protocol [26].

Position of the capsule	Length Range (cm)	Preset flux/ncm^{-2}s^{-1} at half power (17 kW)	Irradiation Protocol	Irradiation Time/s
Bottom	0 to 5	5.0×10^{11}	The set of capsules labeled "bottom_bare & bottom_Cd" containing the prepared flux monitors was sent in turns into the reactor for both bare and cadmium covered respectively.	5400
Middle	5 to 10	5.0×10^{11}	An empty capsule filled with cotton wool and heat sealed was first sent in each case followed in turns by the capsules labeled "middle bare & midlle_Cd" containing the prepared flux monitors for both bare and cadmium covered respectively.	5400
top	10 to 15	5.0×10^{11}	Two empty capsules filled with cotton wool and heat sealed were first sent followed by the capsule labeled "top_bare & top_Cd" containing the prepared flux monitors for both bare and cadmium covered respectively	5400

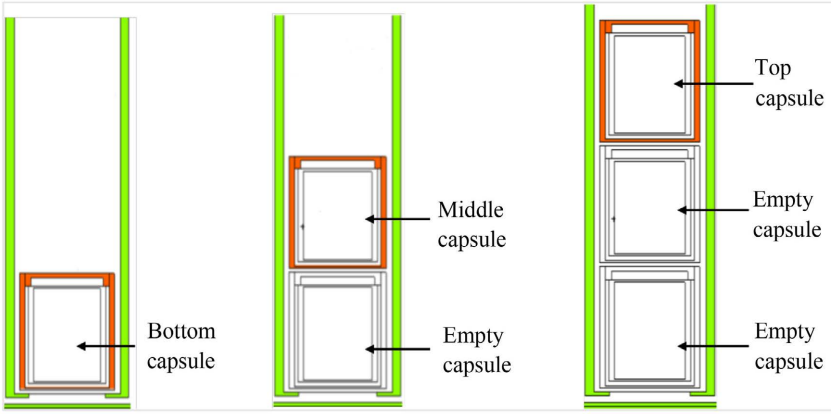

Figure 2. Multi-capsule irradiation protocol [26].

3.2. MCNP Simulation

Neutronic simulations of the present case was conducted by using MCNP5 and the input deck used was that employed for the study conducted by Osei [3]. Modifications were implemented in the deck to reflect the GHARR-1 current LEU core. The part of the model of interest in this study was the inner irradiation channel which was modified in various ways to suit the experimental protocol in this study. The inner irradiation site was modified by discretising its axial length into spatial demarcations for Bottom, Middle and Top Capsules as shown in **Figure 3**.

One of the targets of the MCNP simulation was to replicate the experimental process performed at the inner irradiation site. For bare irradiation, three rabbit capsules were modelled inside the LEU inner column and for cadmium cover irradiation, three cadmium cylinders and bare capsules were modelled inside the irradiation channel as in **Figure 3**. This modification was necessary for the simulation of the Cadmium ratios of the activated foils (Au and Zr), f and alpha (α)-values and the neutron fluxes across each volume of the capsules.

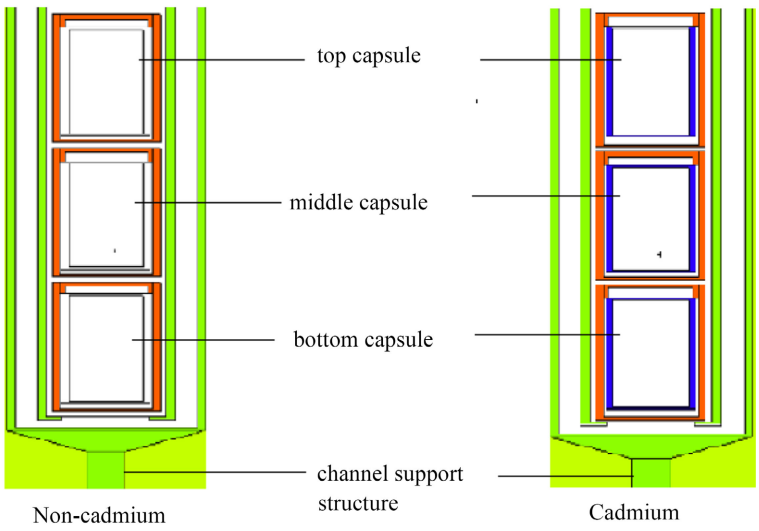

Figure 3. Capsules modelled inside the LEU Inner irradiation channel for bare and cadmium covered.

Additional analysis conducted with the MCNP simulation is the comparison of neutron spectrum characteristics of MNSR LEU and the HEU core. The comparison covered thermal, epithermal, and fast neutron characteristics using 3 energy groups and 400 neutron energy bins. The tally multiplier card (FMn) and the cell flux tally card (F4: N) were combined for the normalization of the flux tallies respectively. The MCNP model was simulated by employing MCNP's criticality card (KCODE): 100000 particles per cycle, 330 cycles with first 30 cycles skipped, and an initial k_{eff} guess of 1.004. The Monte Carlo statistical error in each calculation was less than 1%. The ENDF-B/V and ENDF-B/VI cross-section data libraries were used in all cases.

In modelling of the GHARR-1 using MCNP simulation code, the cell cards, surface cards and data cards were used to model the structures and components of the reactor core. The structures and components modelled include fuel pins/elements, top and lower end plugs of the fuel pins, beryllium reflectors, top and bottom grid plates, control rod, control rod guide tube, top and lower water orifices, fission chambers, aluminum support structure (aluminum support structures below and above reflectors), temperature transducer, inner and outer irradiation channels, reactor vessel, planes for rabbit capsules, air column in reactor vessel, top cover plate of the reactor vessel, slant tube, reactor pool, and reactivity regulating rods (refer to **Figure 1**). The materials modelled using data cards include control rod cadmium metal, stainless steel clad, polyethylene rabbit capsule, guide tube aluminum matrix, guide tube water, reactor core coolant water, reactor pool coolant water, top grid plate zirconium, uranium 235 13% fuel, beryllium reflectors, and activation materials such as Au-197, Zr-94, Zr-96, Mn-55, Al-27, Fe-58, Lu-176, Co-56, Sc-45 and W-186. The input file can be modified to suite several calculation purposes such as criticality, flux, reactivity, reactivity coefficients, delayed neutron fraction, neutron generation time and control rod worth calculations. The additional cards such as cell flux tally (Fn), tally segment (FSn), tally multiplier (FMn) and tally energy (En) cards were used to model other necessary information required and related to the reactor core.

3.2.1. Determination of Reactor Neutron Parameters Using MCNP Simulation

To determine the neutron spectrum parameters (f and alpha (α)-value) across each volume of the three capsules modelled, Gold and Zirconium foils were used. The Cadmium ratio (R_{Cd}) of the foils (Au and Zr) activation based on the reactions ($^{197}Au(n, \gamma)^{198}Au$ and $^{94}Zr(n, \gamma)^{95}Zr$) was determined as the ratio of the bare foil activation to the cadmium covered. A factor of one (1) for the cadmium transmission factor (F_{Cd}) was assumed. The f and α values were obtained using the same approach as performed in the experimental f and α determination [1] [2]. However, in determining the neutron fluxes across the volume of each of the capsules modelled, an energy group was specified to track the flux of neutrons across the volume of each capsule. **Table 3** shows the specified energy groups used.

Table 3. Neutron spectrum energy ranges.

Neutron spectrum region	Energy range
Thermal neutrons	0 - 5.5E−7 MeV
Epithermal neutrons	5.5E−7 - 1.0E−1 MeV
Fast neutrons	1.0E−1 - 20.0 MeV

Using the F4: N (track length estimates of cell flux) card, the neutron fluxes within the volume of each capsule were simulated. However, outputs of MCNP neutron flux are in per cm^2. To convert these fluxes into conventional neutron flux in neutrons per cm^2 per sec ($ncm^{-2}s^{-1}$), a normalization factor (N_f) was established. This factor is dependent on the reactor power and the number of neutrons per fission. Equation (1) and Equation (2) illustrate how this factor was calculated.

$$\left(\frac{1\text{ joule}/\sec}{\text{watt}}\right)\left(\frac{1\text{ MeV}}{1.6\times10^{-13}\text{ Joules}}\right)\left(\frac{\text{Fission}}{180\text{ Mev}}\right)=3.467\times10^{10}\frac{\text{Fission}}{\text{watt sec}} \quad (1)$$

$$N_f=3.467\times10^{10}\frac{\text{fission}}{\text{watt sec}}\times P\text{ watt}\times\bar{\nu}\frac{\text{neutrons}}{\text{fission}} \quad (2)$$

$$N_f=3.467\times10^{10}\times P\times\bar{\nu}\,\text{neutrons/fission}$$

where P is the steady state reactor power, and in this work, reactor power of 17000 W was maintained throughout. 180 MeV is the energy release per fission in both LEU and HEU cores.

Aside from the neutron fluxes determined across the three capsules that were modelled using the three neutron energy groups, a simulation to determine the whole neutron spectrum using 400 neutron energy bins across the three capsules modelled for the bare and cadmium cover was performed. This was significant for ascertaining the neutron fluxes determined using the three neutron energy groups across the three capsules (bottom, middle and top). Another aspect of this simulation was to determine the characteristic effect of the cadmium on the neutron spectrum by modelling the condition (*i.e.*, the cadmium capsule) in the MCNP.

3.2.2. HEU and LEU Neutronic Characteristics Using MCNP Simulations

To compare the neutronics of the HEU and LEU cores, two major simulations (*i.e.*, axial neutron flux and the whole neutron spectrum) were performed for both the HEU and LEU models for the inner and outer irradiation columns as depicted in **Figure 4** and **Figure 5**. In **Figure 4**, the irradiation columns were equally divided into ten planes using the Fs card and based on the En card, three neutron energy groups as specified in **Table 3** was considered. Also, the energy groups: 0 - 6.25E−7, 6.25E−1 - 8.21E−1 and 8.21E−1 - 20 MeV for the thermal, epithermal and fast neutrons respectively were also considered.

Also, in **Figure 5**, the whole volume of the irradiation columns (*i.e.*, HEU and LEU inner and outer) was simulated by employing the En tally card with arbitrary 400 neutron energy (MeV) bins.

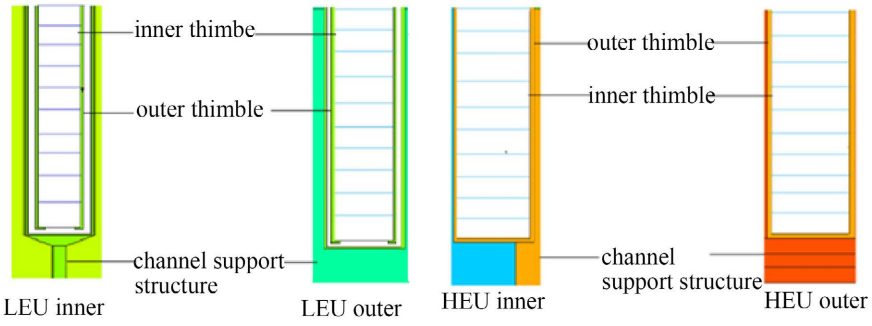

Figure 4. LEU and HEU inner and outer irradiation columns segmented into ten planes.

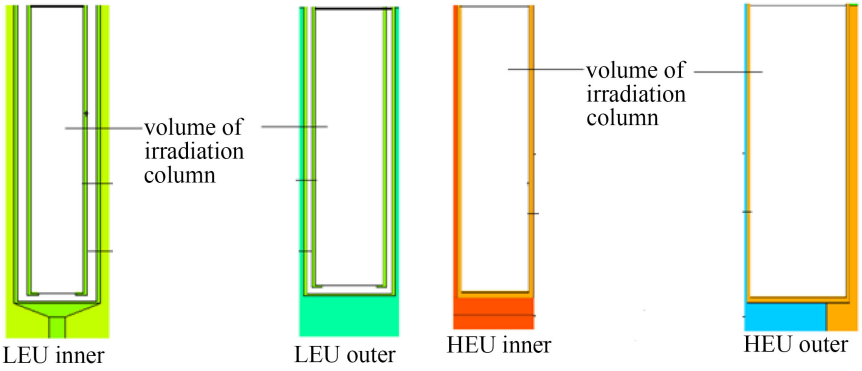

Figure 5. LEU and HEU inner and outer irradiation columns-whole volume.

4. Results and Discussion

Neutron Spectrum Parameters

The neutron spectrum parameters such as the Cadmium ratios (R_{Cd}), the measure of the deviation of epithermal neutrons from the ideal 1/E distribution (α), the thermal-epithermal flux ratio (f), the thermal, epithermal and fast neutron fluxes were determined inside each irradiation capsule positioned at the bottom, middle and top in the inner irradiation channel as presented in Table 4 for both experimental determination and MCNP simulations.

The results obtained for the bottom capsule were compared with similar experiments performed by [23] and [27] and simulations performed by [3].

Table 4. Comparison of neutron flux characterization parameters in the inner irradiation channel at bottom, middle and top capsule positions.

Capsule Position	Reference	R_{cd}		f	α	ϕ_{th} (ncm^{-2}s^{-1})	ϕ_{epi} (ncm^{-2}s^{-1})	ϕ_f (ncm^{-2}s^{-1})
		^{97}Au	^{94}Zr					
Bottom Capsule	EXP. (Adu-Okyere *et al.* [26])	2.21	3.00	18.5 ± 3.7	−0.096 ± 0.029	$4.6 \times 10^{11} \pm 1.11 \times 10^{10}$	$2.49 \times 10^{10} \pm 5.98 \times 10^{8}$	$9.24 \times 10^{10} \pm 2.2 \times 10^{9}$
	EXP. (Baidoo *et al.* [27])	2.08	3.45	18.8	−0.048	5.12×10^{11}	2.47×10^{10}	2.49×10^{10}
	EXP. (Osei *et al.* [23])	2.02	3.51	16.8	−0.039	5.02×10^{11}	2.98×10^{10}	10.4×10^{10}

Continued

	MCNP (Present Work)	2.02	2.16	18.8 ± 3.76	−0.100 ± 0.003	6.86×10^{11} $\pm 3.3 \times 10^{10}$	5.04×10^{11} $\pm 2.5 \times 10^{10}$	3.15×10^{11} $\pm 2.6 \times 10^{10}$
	MCNP (Osei [3])	1.96	2.59	17.8	−0.097	6.44×10^{11}	5.25×10^{11}	3.23×10^{11}
Middle Capsule	EXP. (Adu-Okyere *et al.* [26])	2.10	2.06	21.0 ± 4.2	−0.18 ± 0.036	4.21×10^{11} $\pm 1.01 \times 10^{10}$	2.01×10^{10} $\pm 4.82 \times 10^{8}$	4.81×10^{10} $\pm 1.15 \times 10^{9}$
	MCNP (Present Work)	2.13	3.12	17.9 ± 3.58	−0.078 ± 0.023	6.74×10^{11} $\pm 3.37 \times 10^{10}$	4.96×10^{11} $\pm 2.48 \times 10^{10}$	3.22×10^{11} $\pm 1.61 \times 10^{10}$
Top Capsule	EXP. (Adu-Okyere *et al.* [26])	2.63	2.04	23.0 ± 7.08	−0.20 ± 0.06	3.90×10^{11} $\pm 9.36 \times 10^{9}$	1.65×10^{10} $\pm 3.90 \times 10^{8}$	4.82×10^{10} $\pm 1.16 \times 10^{9}$
	MCNP (Present Work)	2.43	3.09	19.1 ± 3.82	−0.11 ± 0.033	5.94×10^{11} $\pm 2.97 \times 10^{10}$	3.48×10^{11} $\pm 1.74 \times 10^{10}$	2.29×10^{11} $\pm 1.15 \times 10^{10}$

R_{Cd}: Cadmium ratio; α: Measure of the deviation of epithermal neutrons from the ideal 1/E distribution; f: Thermal-epithermal neutron flux ratio; ϕ_{th}: Thermal neutron flux ($ncm^{-2}s^{-1}$); ϕ_{epi}: Epithermal neutron flux ($ncm^{-2}s^{-1}$); ϕ_f: Fast neutron flux ($ncm^{-2}s^{-1}$).

The MCNP simulation results agree quite well with the results presented by [3] within a relative deviation of 3% - 14%. Marginal deviations were also observed in all neutronic parameters measured for the modelled LEU core. It is therefore a fair conclusion that the protocols employed for the spectrum characterization in the present work were adequate. Additional comparison between the experimental results and the MCNP simulations in this work show varying degrees of deviations (4% - 30%) for the Cadmium ratios, f and alpha values. Large deviations (30% - 95%) were observed for the neutron spectrum parameters (thermal, epithermal and fast flux).

The observed deviations in the experimental results compared to the MCNP results shown in **Table 4** are largely attributed to the state of the rector cores (*i.e.*, the actual reactor core and MCNP core). The experimental results depict the exact state of the reactor core (*i.e.*, its physics characteristics at the time of the experiments, after 5 years of operation of the LEU core which was installed in July 2017). However, unlike the experiment, the MCNP input deck depicts the fresh core without considering the compositional changes of the Uranium isotopes, moderator, the core structural materials including burnup corrections or build-up of Xenon and Samarium poison, hence the observed deviations. In addition, the reactor is filled with reactivity insertion materials (cadmium) in some of its irradiation channels due to entrenched reactor safety protocols and irradiation process safety requirements which might have also contributed to the observed deviations in the experimental results compared to the MCNP simulation results.

MCNP Simulation of the whole neutron spectrum for non-cadmium covered and cadmium covered, bottom, middle and top irradiation capsules using an arbitrary 400 neutron energy bins shows neutron spectrum depicted in **Figure 6** and **Figure 7**.

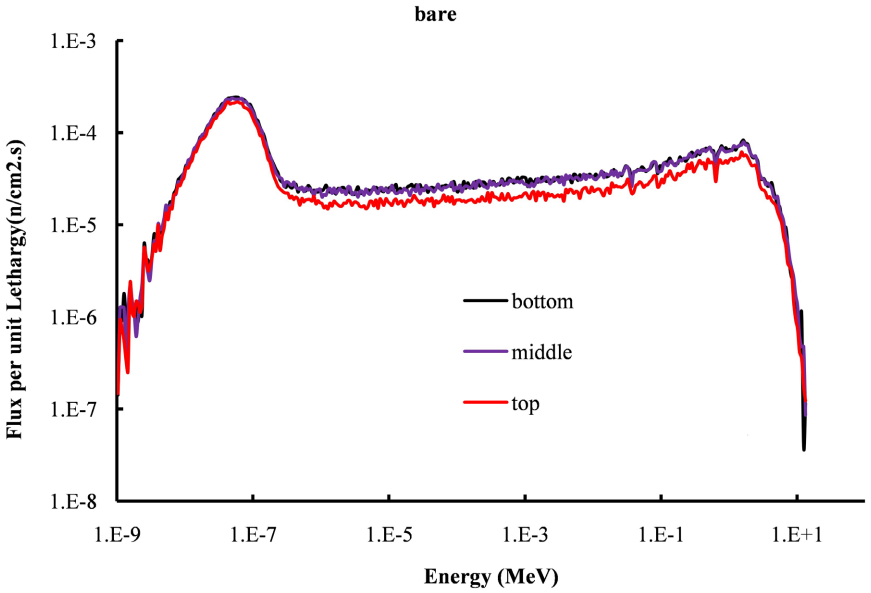

Figure 6. Comparison of the neutron flux spectrum for non-cadmium covered (Bare) capsules (Bottom, middle and top).

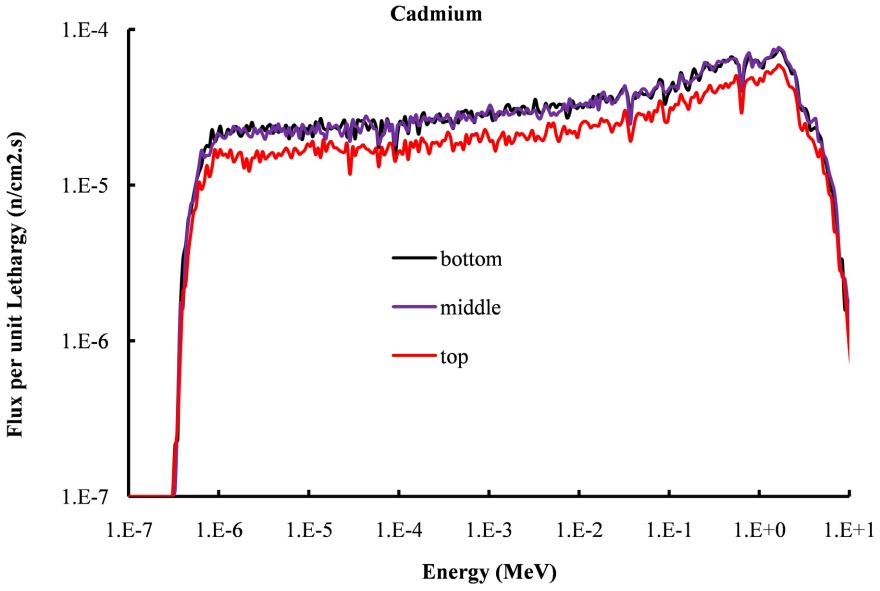

Figure 7. Comparison of the neutron flux spectrum for cadmium covered capsules (Bottom, middle and top).

Figure 6 and Figure 7 represent typical thermal reactor neutron spectra. The vertical axis of the graph represents the flux per unit lethargy and the horizontal axis also represents the logarithmic of the neutron energy [28]. Relative to the core, the neutron flux decreases from the bottom across the top.

No significant differences in trend across the thermal and fast energy spectrum were observed for the bottom, middle and top irradiation capsules as in Figure 7. However, significantly higher flux per unit lethargy were observed at the bottom and middle irradiation capsule positions than for the top irradiation capsule po-

sition. This is an indication that, as neutrons moves further away from the active reactor core, only energetic neutrons are able to tunnel through and hence the relatively high thermal neutron flux and also relatively lower f-value observed for the bottom capsule as compared to the middle and top capsules.

Trend of energy spectrum for the case of cadmium covered capsules as shown in **Figure 7** is distinct from that of non-cadmium covered capsules in **Figure 6**. The energy spectrum for the cases of cadmium covered capsules is observed to begin at much higher value (1.0E−7 MeV) than for non-cadmium covered cases (1.0E−9 MeV). This suggests a neutron spectrum cut-off in the range (1.0E−9 MeV)~(1.0E−7 MeV) and hence confirms a cadmium cut-off energy of 5.5E−7 MeV (0.55 eV) [5]. The results further indicate that neutrons within the energy range from 0 MeV to approximately 1.0E−7 MeV do not contribute to sample activation for irradiation performed under cadmium covered (*i.e.*, placement of cadmium around the activation foils or samples during irradiation).

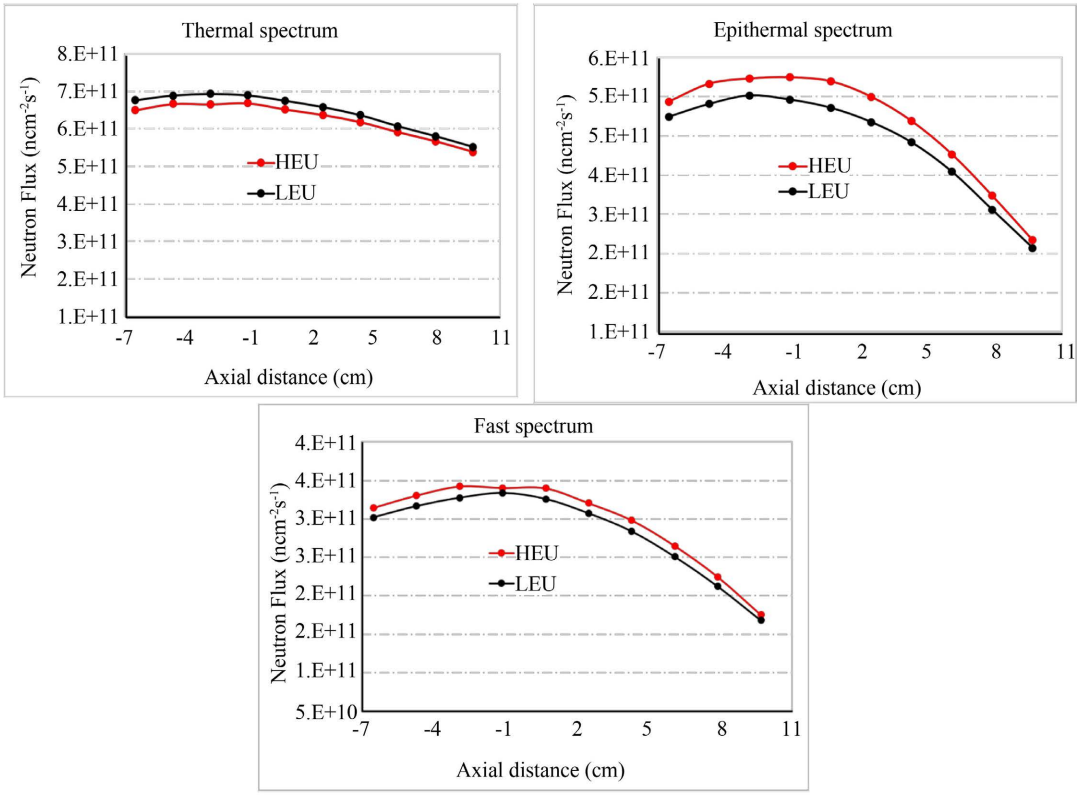

Figure 8. Comparison of axial flux profile of three neutron energy group (0 - 5.5E−7, 5.5E−7 - 1.0E−1 and 1.0E−1 - 20 MeV) for the HEU and LEU inner irradiation site.

Axial neutron flux profile and the distribution of whole neutron energy spectrum within the inner and outer irradiation columns of HEU and the LEU core were determined to ascertain the variations or similarities in the neutronic characteristics of the two reactor cores. The axial neutron flux distribution for the HEU and LEU models were determined using three neutron energy groups. Two sets of neutron energy groups were considered: one set is those typically found in

literature for cadmium cut-off and the other is a default three-energy group associated with the MNSR MCNP input. The energy groups (*i.e.*, typical cadmium cut-off energy in literature) ranged from 0 - 5.5E−7, 5.5E−7 - 1.0E−1 and 1.0E−1 - 2.0E1 [29] and the other set of neutron energy groups (*i.e.*, MNSR MCNP input) also ranged from 0 - 6.25E−7, 6.25E−7 - 8.21E−1 and 8.21E−1 - 2.0E1 MeV [12], [30] respectively for thermal, epithermal and fast neutrons.

Figure 8 and Figure 9 compare the inner irradiation channel spectrums of the two set neutron energy groups (0 - 5.5E−7, 5.5E−7 - 1.0E−1 and 1.0E−1 - 2.0E1) MeV and (0 - 6.25E−7, 6.25E−7 - 8.21E−1 and 8.21E−1 - 2.0E1) MeV.

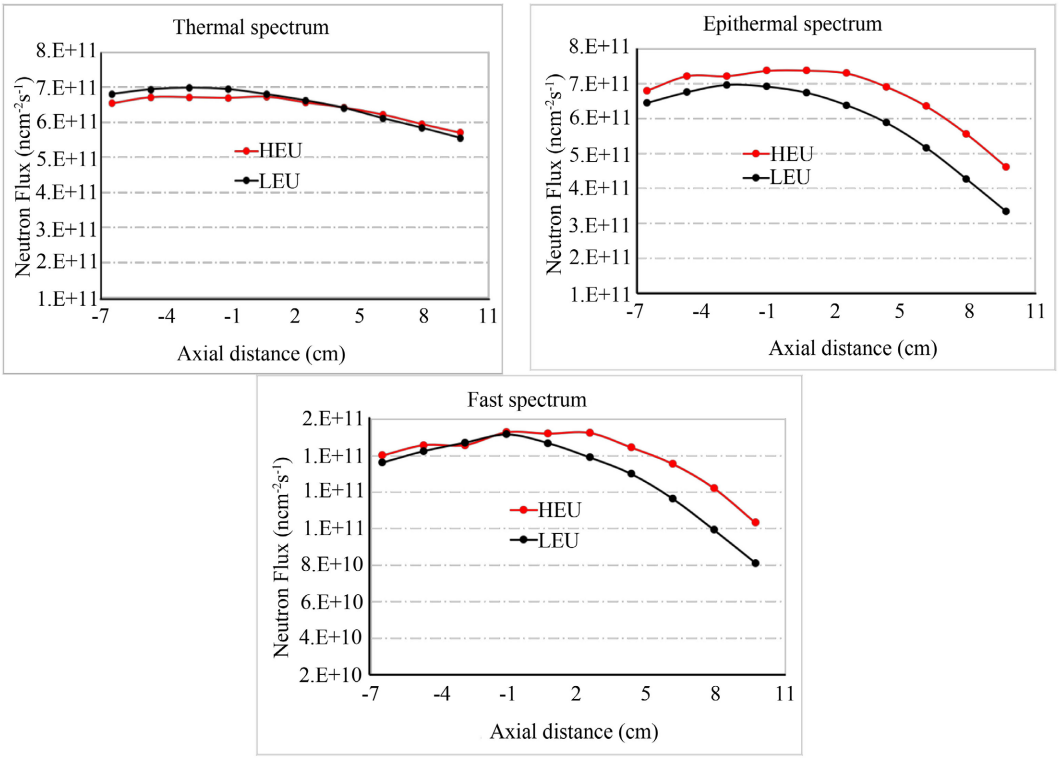

Figure 9. Comparison of axial flux profile of three neutron energy group (0 - 6.25E−7, 6.25E−7 - 8.21E−1 and 8.21E−1 - 20 MeV) for the HEU and LEU Inner Irradiation Site.

For both HEU and LEU modelled cores, similar trend in neutron spectrum is observed and a characteristic drop in neutron flux realised for axial movement away from the core. Significant variation in thermal spectrum corresponding to the neutron energy, 0 - 5.5E−7 could be observed with clear distinction between the HEU and LEU thermal spectrums. Although neutron spectrum trend of the LEU core over-predicts the HEU neutron spectrum within the axial length range of (−7 to 0) cm, the two profiles merges beyond this range. For the spectrum (5.5E−7 to 1.0E−1 and 1.0E−1 to 2.0E1), the curve converges as you move down along the core. In the case of (6.25E−7 to 8.21E−1 and 8.21E−1 to 2.0E1), the curve diverges. The two figures (Figure 8 and Figure 9) show the importance of presenting the two set of energy groups. With the slight variation in the boundaries of the energy group in the entire neutron spectrum in the inner irradiation channel, the neutron flux profiles change.

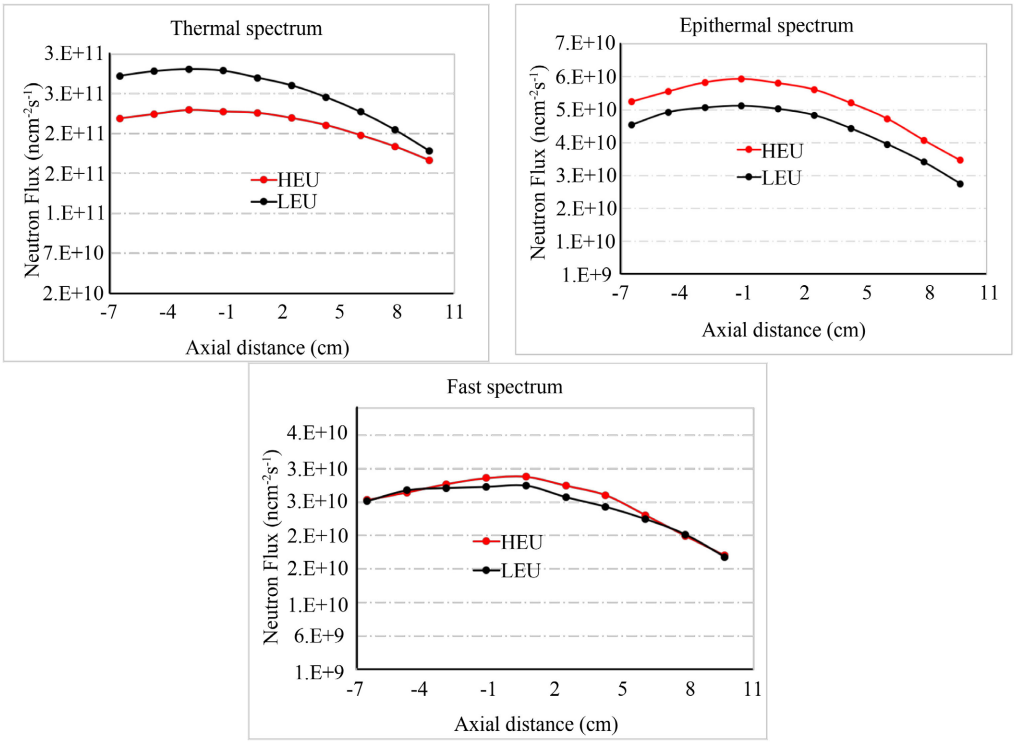

Figure 10. Comparison of axial flux profile of three neutron energy group (0 - 5.5E−7, 5.5E−7 - 1.0E−1 and 1.0E−1 - 20 MeV) for the HEU and LEU Outer Irradiation Sites.

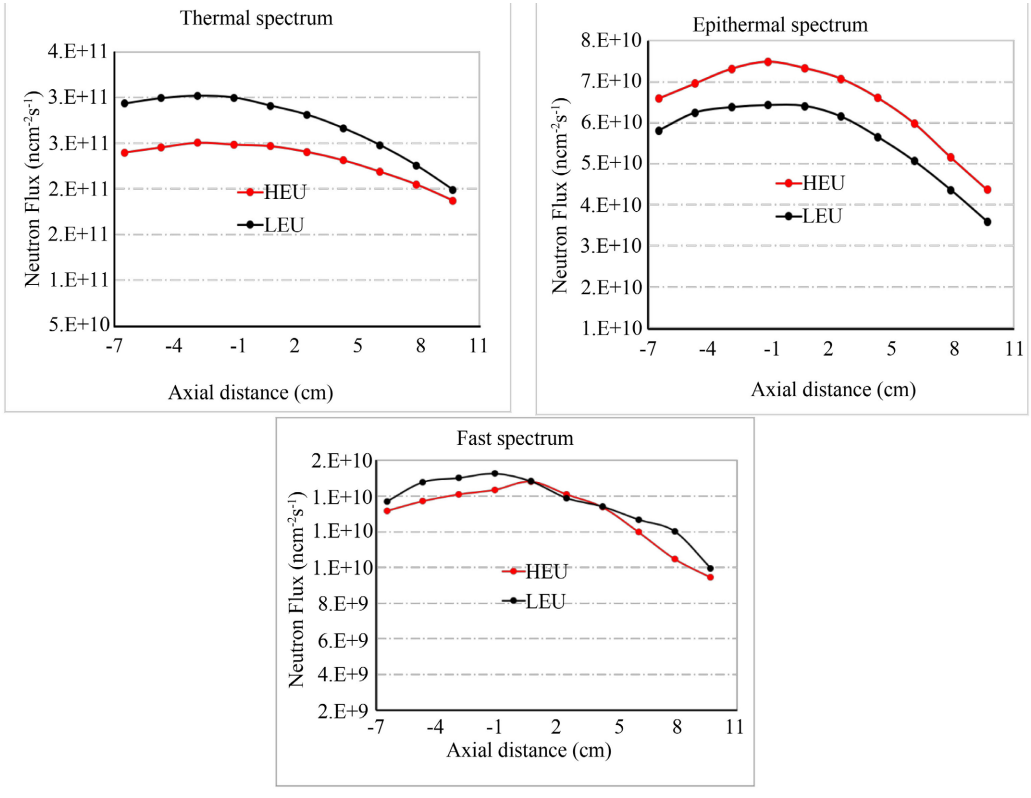

Figure 11. Comparison of axial flux profile of three neutron energy group (0 - 6.25E−7, 6.25E−7 - 8.21E−1 and 8.21E−1 - 20 MeV) for the HEU and LEU Outer Irradiation Site.

Figure 10 and Figure 11 also compare the outer spectrums for the two set neutron energy groups (0 - 5.5E−7, 5.5E−7 - 1.0E−1 and 1.0E−1 - 2.0E1) and (0 - 6.25E−7, 6.25E−7 - 8.21E−1 and 8.21E−1 - 2.0E1 MeV).

No significant differences are observed in the spectrum trend for the two set energy groups (0 - 5.5E−7, 5.5E−7 - 1.0E−1 and 1.0E−1 - 2.0E1) MeV and (0 - 6.25E−7, 6.25E−7 - 8.21E−1 and 8.21E−1 - 2.0E1) MeV considered for the MCNP simulation.

Thermal spectrum in both the inner and outer channels was observed to be relatively high for the LEU compared to the HEU. The high thermal spectrum for the LEU is also observed in [3] when the HEU and LEU flux at half power was compared (*i.e.*, HEU at 15 kW and LEU at 17 kW). It must be noted that the previous HEU core was a 30 kW power reactor, however, the current LEU core operates at the maximum power of 34 kW. This account for the relative increase in the thermal spectrum of the LEU due to the increase in thermal power (*i.e.*, from 30 to 34 kW) to make up for the thermal neutron trade-off for the LEU core as a result of the core conversion from HEU to LEU.

Results of the whole volume simulations of the inner and outer irradiation sites for both HEU and LEU cores using 400 arbitrary neutron energy bins are shown in Figure 12 and Figure 13.

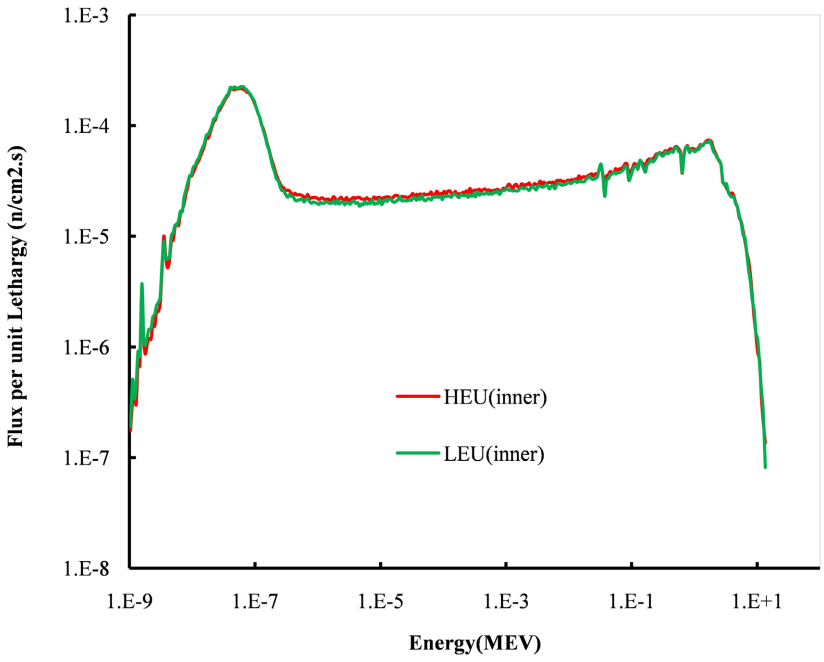

Figure 12. Comparison of the neutron flux and energy for the HEU and LEU inner irradiation site.

Identical neutron spectrums characteristics are observed for the whole volume, inner and outer irradiation sites simulations. The similar spectrums observed are largely due to the retained dimension of the HEU and some other materials like the coolant/moderator etc., with the only changes being the material composition

and percentage of fuel (90.2 - 13.0 wt. % of U-235), control rod and its guide tube [3] [31]. According to the findings, the impact of operation or utilization concerning neutron spectrum parameters in irradiation channels has minimal or negligible influence as a result of a commercial MNSR conversion. In essence, the choice between HEU and LEU in reactor design involves tradeoffs between core size, fuel loading, neutron flux, and the complexity of achieving and maintaining criticality. HEU and LEU differ primarily in the concentration of the fissile isotope Uranium-235 (U-235), and this significantly affects reactor physics parameters and operational characteristics/behaviors related to neutron cross-sections.

Similar to this work, a feasibility research was performed by [32] for generic MNSR LEU fuels to predict the impact of a possible core conversion from HEU to LEU. The results suggested that a core fueled by UO_2 fuel with 12.5% enrichment would reproduce the same neutronics data as the HEU core with 90.2% enrichment [33] [34]. This was ascertained by [31] prior to the NIRR-1 core conversion where a neutronic study was conducted to access the impact of HEU to LEU. The results obtained indicated similar neutron spectrums distribution for both HEU and the LEU. The axial distribution of the neutron spectrum, in all cases (*i.e.*, both inner and outer) also showed a relatively high spectrum at the thermal neutron region (*i.e.*, 1.0E−9 to 1.0E−7 MeV approximately) for the LEU with minimal marginal difference compared to the HEU. From the criticality calculation, the keff obtained is 1.0034 for LEU and 1.0032 for HEU.

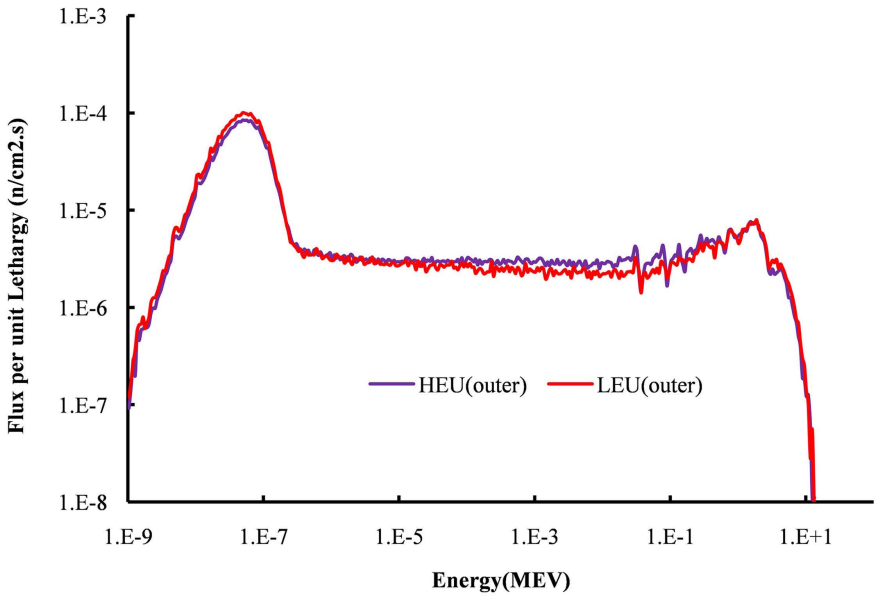

Figure 13. Comparison of the neutron flux and energy for the HEU and LEU outer irradiation site.

The single capsule irradiation channel protocols have been developed and adopted over the years during the operation of the HEU core. The reactor core is currently operated with the LEU core as a result of conversion of the HEU core to

the LEU core. It is necessary to compare the LEU MCNP simulations with the HEU MCNP simulations to see whether there would be significant deviations between the results obtained on three energy groups (thermal, epithermal and fast fluxes) as shown in **Figures 8-11** as well as the flux versus energy results shown in **Figure 12** and **Figure 13**. The reaction rate equations and neutron flux equations for the neutron fluxes in the three different energy groups (thermal flux, epithermal flux and fast flux) can be found in the references [3] [23] [26] and many other references in the literature. Flux characterization protocols developed for HEU experimental study by Baidoo *et al.* [27], and this experimental study results [27] have been used to validate the HEU MCNP simulation studies. Similar LEU flux characterization protocols have been developed to obtain the experimental results by Adu-Okyre *et al.* [26], which have been used to validate the MCNP results in this study. The observed significant variation observed between the LEU experimental study [26] and this study is partly due to the fact that the MCNP simulation has not replicated the multi-capsule experimental set-up exactly the manner in which the multi-capsule experiment was carried out (**Table 4**), and also partly due to the MCNP simulation unable to simulate the exact state of the core as explained in the text earlier (the compositional changes of the Uranium isotopes, moderator, the core structural materials including burnup corrections or build-up of Xenon and Samarium poison, as well as the addition of reactivity insertion material in some of the irradiation channels contributed to the observed deviations. The burnup of the fissile content (U235) of the fuel over the years of the reactor operation results in the reduction of the expected neutron flux level (or power level). Reduction in the neutron flux level (or power level) below certain level can shut down the reactor during reactor operation). The MCNP simulated all the bare samples together and all the Cadmium-covered samples together. The multi-capsule experiment was carried out by activating each sample separately. Because of the high neutron capture characteristics of Cadmium, activating all the 3 Cadmium-covered samples together would shut down the reactor. However, there is agreement between the MCNP single-capsule HEU and LEU simulation results (**Figures 8-11**). Also there is agreement between flux versus energy results presented in **Figure 6** and **Figure 12**, the MCNP inner-irradiation results with extension to multi-capsule simulation (**Figure 6**). Based on this general agreement between the results obtained, the LEU flux characterization protocols developed for the LEU multi-capsule experimental study are adequate for the GHARR-1 facility to be used for multi-capsule irradiation of long and intermediate radionuclides.

5. Conclusions

Monte Carlo N-Particle Transport (MCNP) simulation was employed in the present work to theoretically mimic an experimental study on flux characterization in which a multi-capsule scheme realised through the introduction of three (3) irradiation capsules each of length 5 cm into the 17 cm long irradiation channel of the Ghana Research Reactor 1 (GHARR-1) facility. The objective was to provide

a sound scientific basis for extending the accessible irradiation space, especially for irradiation involving intermediate and long lived radionuclides by 60% during the utilization of the Ghana Research Reactor 1 (GHARR-1) facility. The routine characterisation of the GHARR-1 inner irradiation channel is conducted by the introduction of a single irradiation capsule (5 cm long) loaded, underutilising the available irradiation space in the inner irradiation channel. Of interest to the objectives of the present work is also, the characterization of neutron spectrum and determination of their spatial distribution close to the full length of the inner irradiation channel and also to conduct a comprehensive neutronics simulation to analyse the neutronics characteristics and impact of the conversion from HEU to LEU core on the neutron spectrum using MCNP. The GHARR-1 MCNP input deck was modified in the present work to suit the discretisation of the inner irradiation channel required for the present work and to support the multi capsule irradiation protocol which was investigated. The whole neutron spectrum of the HEU and LEU inner and outer columns was determined using 400 arbitrary neutron energy bins. The HEU and LEU axial neutron flux variation was determined using three energy groups respectively for the thermal, epithermal and fast neutron spectrum. Experimental results obtained show increasing f-value across the irradiation column as, 18.5 ± 1.7, 21.0 ± 2.2 and 23.0 ± 7.08 respectively from the bottom capsule to the top capsule; the MCNP simulation results are 18.8 ± 3.76, 17.9 ± 3.58 and 19.1 ± 3.82 respectively from the bottom capsule to the top capsule. The corresponding epithermal neutron shaping factor (α-value) varied as, −0.096 ± 0.029, −0.18 ± 0.036 and −0.20 ± 0.06 from the bottom to the top capsule respectively; the MCNP simulation results are −0.100 ± 0.003, −0.078 ± 0.023 and −0.11 ± 0.033 from the bottom to the top capsule respectively. The respective experimental results determined in the bottom capsule irradiation column for thermal, epithermal and fast fluxes are $4.60 \times 10^{11} \pm 2.5 \times 10^{10}$, $2.49 \times 10^{10} \pm 5.98 \times 10^{8}$, $9.24 \times 10^{10} \pm 2.2 \times 10^{9}$; the MCNP simulation results are $6.86 \times 10^{11} \pm 3.4 \times 10^{10}$, $5.04 \times 10^{11} \pm 2.5 \times 10^{10}$, $3.15 \times 10^{11} \pm 2.6 \times 10^{10}$. The respective experimental results determined in the middle capsule irradiation column for thermal, epithermal and fast fluxes are $4.21 \times 10^{11} \pm 1.01 \times 10^{10}$, $2.01 \times 10^{10} \pm 4.82 \times 10^{8}$, $4.81 \times 10^{10} \pm 1.15 \times 10^{9}$; the MCNP simulation results are $6.74 \times 10^{11} \pm 3.3 \times 10^{10}$, $4.96 \times 10^{11} \pm 2.48 \times 10^{10}$, $3.22 \times 10^{11} \pm 2.6 \times 10^{10}$. The respective experimental results determined in the top capsule irradiation column for thermal, epithermal and fast fluxes are $3.90 \times 10^{11} \pm 9.36 \times 10^{9}$, $1.65 \times 10^{10} \pm 3.90 \times 10^{8}$, $4.82 \times 10^{10} \pm 1.16 \times 10^{9}$; the MCNP simulation results are $5.94 \times 10^{11} \pm 2.97 \times 10^{10}$, $3.48 \times 10^{11} \pm 1.74 \times 10^{10}$, $2.29 \times 10^{11} \pm 1.15 \times 10^{10}$. The MCNP Neutronic simulation results indicated similar HEU and LEU spectrum characteristics suggesting very minimal or negligible impact of the HEU to LEU core conversion on the neutron spectrum parameters.

Acknowledgements

The authors acknowledge the technical supports from Scientists and Technicians at the Ghana Research Reactor-1 (GHARR-1) facility of the Ghana Atomic Energy

Commission (GAEC).

Conflicts of Interest

The authors declare no conflict of interest with respect to the submitted manuscript for publication.

References

[1] Borio di Tigliole, A., Cammi, A., Clemenza, M., Memoli, V., Pattavina, L. and Previtali, E. (2010) Benchmark Evaluation of Reactor Critical Parameters and Neutron Fluxes Distributions at Zero Power for the TRIGA Mark II Reactor of the University of Pavia Using the Monte Carlo Code MCNP. *Progress in Nuclear Energy*, **52**, 494-502. https://doi.org/10.1016/j.pnucene.2009.11.002

[2] Hamidatou, L. and Benkharfia, H. (2010) Experimental and MCNP Calculations of Neutron Flux Parameters in Irradiation Channel at Es-Salam Reactor. *Journal of Radioanalytical and Nuclear Chemistry*, **287**, 971-975. https://doi.org/10.1007/s10967-010-0922-9

[3] Osei, B. (2017) Characterization of Ghana Research Reactor-1 Low-Enriched Uranium Core Irradiation Sites using a Theoretical Method. Ph.D. Thesis, University of Ghana. http://ugspace.ug.edu.gh/handle/123456789/23631

[4] Briesmeister, J.J. (2005) MCNP5—A General Monte Carlo N-Particle Transport Code, Version 5. Los Alamos National Laboratory.

[5] Brewer, R. (2009) Criticality Calculations with MCNP5: A Primer, LA-UR-09-00380. https://mcnp.lanl.gov/pdf_files/TechReport_2009_LANL_LA-UR-09-00380_Brewer.pdf

[6] Kim, K., Roh, G. and Lee, B. (2022) Characterization of Neutron Spectra for NAA Irradiation Holes in H-LPRR through Monte Carlo Simulation. *Nuclear Engineering and Technology*, **54**, 4226-4230. https://doi.org/10.1016/j.net.2022.06.017

[7] Richardson, B., Castano, C.H., King, J., Alajo, A. and Usman, S. (2012) Modeling and Validation of Approach to Criticality and Axial Flux Profile Experiments at the Missouri S&T Reactor (MSTR). *Nuclear Engineering and Design*, **245**, 55-61. https://doi.org/10.1016/j.nucengdes.2012.01.023

[8] AL-Qahtani, M. and Alajo, B.A. (2020) Impact of Initial MCNP Spectrum Guess on Experiment-Based Neutron Spectrum Determination at Missouri S&T Reactor. *Annals of Nuclear Energy*, **141**, Article ID: 107326. https://doi.org/10.1016/j.anucene.2020.107326

[9] Shim, H., Han, B., Jung, J., Park, H. and Kim, C. (2012) MCCARD: Monte Carlo Code for Advanced Reactor Design and Analysis. *Nuclear Engineering and Technology*, **44**, 161-176. https://doi.org/10.5516/net.01.2012.503

[10] Huston, D.A., Samuleev, P., Kelly, F. and Corcoran, E.C. (2024) Characterization of Flux Distribution in the Pool of the RMC Slowpoke-2. *Applied Radiation and Isotopes*, **207**, Article ID: 111262. https://doi.org/10.1016/j.apradiso.2024.111262

[11] Tiyapun, K., Chimtin, M., Munsorn, S. and Somchit, S. (2015) Validation of the MCNP Computational Model for Neutron Flux Distribution with the Neutron Activation Analysis Measurement. *Journal of Physics: Conference Series*, **611**, Article ID: 012007. https://doi.org/10.1088/1742-6596/611/1/012007

[12] Abrefah, R.G., Anim-Sampong, S., Nyarko, B.J.B., Akaho, E.H.K. and Sogbadji, R.B.M. (2011) Measurement of Neutron Flux Distribution in the Irradiation Channel in the Ghana Research Reactor-1 Using Monte Carlo Method. *Progress in Nuclear*

Energy, **53**, 189-194. https://doi.org/10.1016/j.pnucene.2010.07.002

[13] Abrefah, R.G., Sogbadji, R.B.M., Ampomah-Amoako, E., Birikorang, S.A., Odoi, H.C. and Nyarko, B.J.B. (2010) Design of Epicadmium-Shielded Irradiation Channel of the Outer Irradiation Channel of the Ghana Research Reactor-1 Using MCNP. *Nuclear Engineering and Design*, **240**, 744-746. https://doi.org/10.1016/j.nucengdes.2009.12.016

[14] Rataj, J., Suk, P., Bílý, T., Stefanik, M. and Frýbort, J. (2021) Characterisation of Neutron Field in the Polyethylene Neutron Irradiator. *Applied Radiation and Isotopes*, **168**, Article ID: 109529. https://doi.org/10.1016/j.apradiso.2020.109529

[15] Ghninou, H., Gruel, A., Lyoussi, A., Reynard-Carette, C., El Younoussi, C., El Bakkari, B., et al. (2023) Evaluation of the Cnesten's TRIGA Mark II Research Reactor Physical Parameters with TRIPOLI-4® and MCNP. *Nuclear Engineering and Technology*, **55**, 4447-4464. https://doi.org/10.1016/j.net.2023.07.029

[16] Ferraro, D., Ferrari, I., Hergenreder, D. and Villarino, E. (2022) Safety-Related Parameters Calculation for OPAL Reactor Using MCNP v6.1.0 and ENDF/B-VII.1. *Annals of Nuclear Energy*, **178**, Article ID: 109370. https://doi.org/10.1016/j.anucene.2022.109370

[17] Farouki, I., Malkawi, R. and Marashdeh, S. (2021) Monte Carlo Calculations of Neutron Spectrum Parameters at the JRTR NAA Channels. *Progress in Nuclear Energy*, **134**, Article ID: 103688. https://doi.org/10.1016/j.pnucene.2021.103688

[18] Kuatbek, M., Pierson, B.D., Lyons, S.M., Flaska, M. and Johnsen, A.M. (2023) Characterization of the Fast-Neutron Irradiator and the Fast-Flux Tube Irradiation Fixtures at the Pennsylvania State Breazeale Reactor. *Nuclear Engineering and Design*, **413**, Article ID: 112505. https://doi.org/10.1016/j.nucengdes.2023.112505

[19] Harvey, Z.R. (2010) Neutron Flux and Energy Characterization of a Plutonium-Beryllium Isotopic Neutron Source by Monte Carlo Simulation with Verification by Neutron Activation Analysis. Ph.D. Thesis, University of Nevada, Las Vegas.

[20] Clarno, K.T., Barlow, J.E., Sawyer, T., Scherr, J., Hearne, J. and Tsvetkov, P. (2023) Evaluation of SCALE, Serpent, and MCNP for Molten Salt Reactor Applications Using the MSRE Benchmark. *Radiation Physics and Chemistry*, **207**, Article ID: 110837.

[21] Faghihi, F., Mehdizadeh, S. and Hadad, K. (2006) Neutrons Flux Distributions of the Pu-Be Source and Its Simulation by the MCNP-4B Code. *International Journal of Modern Physics E*, **15**, 737-745. https://doi.org/10.1142/s0218301306004545

[22] Degenaar, H. and Blaauw, M. (2003) The Neutron Energy Distribution to Use in Monte Carlo Modeling of Neutron Capture in Thermal Neutron Beams. *Nuclear Instruments and Methods in Physics Research Section B: Beam Interactions with Materials and Atoms*, **207**, 131-135. https://doi.org/10.1016/s0168-583x(03)00457-9

[23] Osei, B., Baidoo, I.K., Odoi, H.C., Gasu, P.D. and Nyarko, B.J.B. (2021) The Low Enriched Uranium Miniature Neutron Source Reactor (LEU-MNSR) Neutron Spectrum Characterization for K0-inaa. *Nuclear Instruments and Methods in Physics Research Section A: Accelerators, Spectrometers, Detectors and Associated Equipment*, **1005**, Article ID: 165397. https://doi.org/10.1016/j.nima.2021.165397

[24] Shitsi, E., Odoi, H.C., Baidoo, I.K., Amponsah-Abu, E.O., Gyamfi, K., Boafo, E.K., Obeng, H.K., Gasu, P.D., Osei-Mensah, W., Massiasta, W.S. and Quagraine, R.E. (2023) Quality Assurance and Quality Control Programmes of Research Reactor Operation and Utilization at GHARR 1 Facility. *Arab Journal of Nuclear Sciences and Applications*, **56**, 9-18.

[25] Adelfang, P. and Atger, A. (2006) Conversion of Research Reactors from HEU to LEU Fuel. *Fuel Cycle Waste Newsletter*, **2**, 1-16.

[26] Adu-Okyere, G., Agbodemegbe, V.Y., Baidoo, I.K., Odoi, H.C. and Shitsi, E. (2024) Feasibility Study for the Adoption of Multi-Capsule Irradiation Protocol in the Conduct of K0-Based INAA Using the GHARR-1 MNSR. *Radiation Physics and Chemistry*, **216**, Article ID: 111393. https://doi.org/10.1016/j.radphyschem.2023.111393

[27] Baidoo, I.K., Nyarko, B.J.B., Akaho, E.H.K., Dampare, S.B., Sogbadji, R.B.M. and Poku, L.O. (2013) Characterization of Low Power Research Reactor Neutrons for the Validation of K0-Inaa Standardization Based on K0-Iaea Software. *Applied Radiation and Isotopes*, **79**, 85-93. https://doi.org/10.1016/j.apradiso.2013.05.005

[28] Lamarsh, J.R. and Baratta, A.J. (2001) Introduction to Nuclear Engineering, vol. 3. Prentice Hall, 253.

[29] IAEA (1990) Practical Aspects of Operating a Neutron Activation Analysis Laboratory. A Technical Document Issued by the International Atomic Energy Agency.

[30] Baidoo, I.K., Li, B., Yang, Q., Song, J. and Hu, L.Q. (2018) Verification of Supermc for MNSRs Core Analysis: The Case of Ghana Research Reactor-I. *Annals of Nuclear Energy*, **113**, 48-54. https://doi.org/10.1016/j.anucene.2017.10.046

[31] Jonah, S.A., Ibrahim, Y.V., Ajuji, A.S. and Onimisi, M.Y. (2012) The Impact of HEU to LEU Conversion of Commercial MNSR: Determination of Neutron Spectrum Parameters in Irradiation Channels of NIRR-1 Using MCNP Code. *Annals of Nuclear Energy*, **39**, 15-17. https://doi.org/10.1016/j.anucene.2011.08.026

[32] Jonah, S.A., Liaw, J.R. and Matos, J.E. (2007) Monte Carlo Simulation of Core Physics Parameters of the Nigeria Research Reactor-1 (NIRR-1). *Annals of Nuclear Energy*, **34**, 953-957. https://doi.org/10.1016/j.anucene.2007.05.010

[33] Jonah, S.A., Ibikunle, K. and Li, Y. (2009) A Feasibility Study of LEU Enrichment Uranium Fuels for MNSR Conversion Using MCNP. *Annals of Nuclear Energy*, **36**, 1285-1286. https://doi.org/10.1016/j.anucene.2009.05.001

[34] Jonah, S.A., Balogun, G.I., Umar, I.M. and Mayaki, M.C. (2005) Neutron Spectrum Parameters in Irradiation Channels of the Nigeria Research Reactor-1 (NIRR-1) for the K0-NAA Standardization. *Journal of Radioanalytical and Nuclear Chemistry*, **266**, 83-88. https://doi.org/10.1007/s10967-005-0873-8

Highlights

- MCNP simulation used to mimic multi-capsule irradiation experimental study
- Flux characterization parameters determined using MCNP simulation
- Flux parameters determined in the bottom, middle and top irradiation/activation column
- HEU and LEU axial neutron flux variation determined
- MCNP simulation results indicated similar HEU and LEU neutron spectrum characteristics